

# WET SNOW PENDULAR REGIME: THE AMOUNT OF WATER IN RING-SHAPED CONFIGURATIONS

A. Denoth\*  
University of Innsbruck, A-6020, Austria

**ABSTRACT:** The water saturation of a natural snow cover varies, in general, from zero to approximately 20% of the pore volume, whereby two essentially different types of water geometry - pendular mode and funicular mode - can be observed. The pendular mode covers the low-saturation range (typically  $S \leq 7\%$  for old coarse grained Alpine snow) and it is assumed that the water component is arranged in isolated menisci or pendular rings around a contact zone between spheroidal ice grains. However, the water rings or menisci are, thermodynamically, in a very critical - may be in an unstable - configuration. As water rings or menisci represent closed electrically conducting loops, they may be responsible for an induced diamagnetic behaviour of snow, especially in the microwave regime; and this offers a way to measure the amount of water stored in this geometrical configuration. From a careful analysis of the measured dielectric and magnetic permeability in the microwave C to K-bands of moderate wet coarse grained Alpine snow results, that water rings seem only to exist at saturations lower than  $\approx 8\%$ . For saturations exceeding this critical value, water rings begin to merge forming clusters, whereby the number of ring-like geometries decreases in favour of larger but open-ended structures.

**KEYWORDS:** snow physics, snow electromagnetic properties, snow water content

## 1. INTRODUCTION

Snow, as any other porous granular material, has three distinct regimes of water saturation: the pendular regime at low saturations with an isolated water phase and a continuous air path throughout the pore space, the funicular regime at higher saturations with continuous liquid paths throughout the pore space and a more or less isolated and trapped gaseous phase, and the regime of complete saturation (Scheidegger, 1974; Colbeck, 1982). A relative simple method to obtain information on the geometry of the individual components of wet snow (ice grains, air and water) is the measurement of electromagnetic parameters: dielectric function, reflection- and transmission coefficients, or wave propagation function. Data analysis based on an appropriate dielectric mixing model, whereby the model of Polder and van Santen (1946) has proofed its efficiency, allows a geometric characterization of the solid and liquid components in terms of

three-axial ellipsoidal bodies. Various measurement series with snow in different stages of metamorphism indicate a significant change in water geometry at saturations ranging from 7 to approx. 14% of the pore volume (Colbeck, 1982; Denoth, 1982a; Hallikainen et al., 1984). Due to capillary forces and surface tension, water in the pendular saturation regime may exist in the form of isolated spheroids and also menisci around the contact zone of ice grains. Recently, a pore size characterization and a calculation of the water volume contained in menisci has been given by Frankenfield (1996). As water menisci represent closed electrically conducting loops, they may be responsible for an induced diamagnetic behaviour of snow, especially in the microwave regime; and this offers a way to measure the amount of water stored in this special geometrical configuration. Quantitatively, the 'induced' diamagnetism depends on the cross-sectional area of the ring-shaped water bodies: so, grain-size will be a dominant parameter. Indications of the existence of water rings have been reported by Mätzler (1988) and Achammer (1996).

In this study, high precision measurements of complex magnetic permeability in the micro-

---

Corresponding author address: A. Denoth,  
Institute of Experimental Physics, Innsbruck,  
A-6020; email: armin.denoth@uibk.ac.at

wave C- to K-band, 6 up to 16 GHz, are presented.

## 2. METHODS AND MATERIALS

In the current study, a free-space measurement technique is used, with the snow sample placed in between transmitting and receiving horn antennas. Polystyrene lenses have been used with high-gain horn antennas to convert the spherical wavefront to a planar wavefront at the sample location. The principle of operation is shown in Fig.1: H1, H2: horn antennas, SH: sample holder, I, R, T: incident, reflected and transmitted signal, Ref: reference signal for phase measurements.

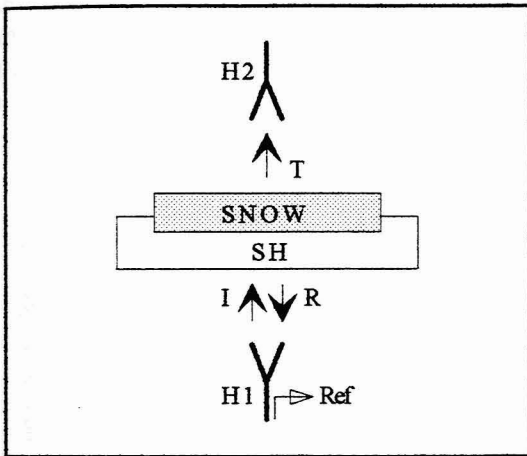


Figure 1. Principle of free-space measurement technique: R-T-method

Additionally - and as a controlling procedure - a standard ellipsometric method (Azzam and Bashara, 1979) has been applied: the reflection coefficients for incident  $\pi$  and  $\sigma$  polarized waves have been measured at  $10^\circ$  incident angle intervals (Brewster-method). The principle of operation is shown in Fig.2: H1, H2: horn antennas, SH: sample holder, I, R: incident and reflected signals.

Magnitude and phase of the reflected and transmitted signals, respectively, are measured with a high-precision computer-controlled network-analyzer, model HP8510A. Frequency of operation is in the 6 up to 16 GHz range. System characteristics (interference effects, signal attenuation) of both the R-T-system and the Brewster-system have been determined by calibration procedures using dielectric test materials of known properties. Based on Fresnel's

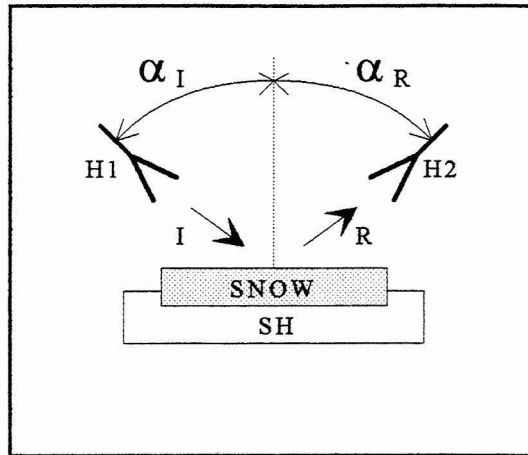


Figure 2. Principle of free-space measurement technique: Ellipsometric method

formulae (Guenther, 1990) snow dielectric permittivity,  $\epsilon = \epsilon' - i\epsilon''$ , and magnetic permeability,  $\mu = \mu' - i\mu''$ , have been deduced from the measured total reflection and transmission coefficients by an iterative technique, whereby multiple beam interference effects within the snow sample have to be considered. Due to the limited accuracy of the measurement system and additional errors introduced by data reduction, the lower measurement frequency has been set to  $f = 6$  GHz.

In contrast to the intrinsic natural diamagnetism, the 'induced' diamagnetism depends on the cross-sectional area of the ring-shaped water bodies (if there are any), and, consequently, depends on the grain size. Therefore, measurements have only be made with coarse up to extremely coarse grained old Alpine snow and firm-type snow. The snow samples selected have been characterized according to wetness ( $W_{tot}$ , [Vol%]), porosity ( $\Phi$ , [%]), and mean grain size ( $r$ , [mm]).  $W_{tot}$ , the total water content, has been measured by a calibrated dielectric probe (Denoth, 1994a; Denoth, 1994b),  $\Phi$  has been calculated from snow density and  $W_{tot}$ , and  $r$  has been derived from a photographic analysis of the individual snow samples (Denoth, 1982b). All the measurements have been carried out in a cold room with controlled ambient temperature, with maximum variations from  $-0.5^\circ\text{C}$  up to  $0^\circ\text{C}$ .

## 3. WET SNOW DIAMAGNETIC FUNCTION

For 5 selected snow samples, typical measurements of magnetic susceptibility,  $\chi = \mu' - 1$ ,

and magnetic loss,  $\mu''$ , in the frequency range from 6 GHz up to 16 GHz are shown in Fig.3a and Fig.3b, respectively. Characteristic data of the snow samples, samples a .... e, are given in Table 1. For sample a, a typical error bar is shown for a frequency of 13 GHz.

sample	$W_{tot}$ [%]	$\Phi$ [%]	$r$ [mm]
a	4.0	46	1.5
b	4.7	52	1.3
c	5.1	46	1.5
d	2.2	47	1.1
e	2.0	48	0.7

Table 1. Characteristic data of 5 selected snow samples

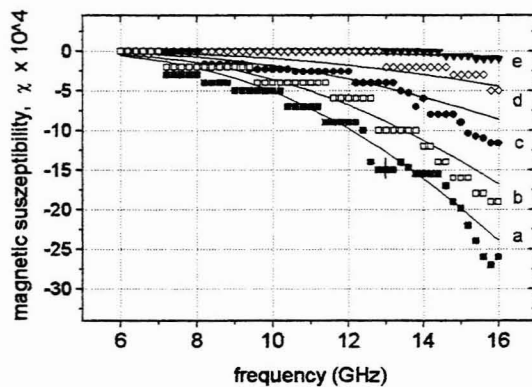


Figure 3a. Frequency dependence of magnetic susceptibility for 5 selected snow samples

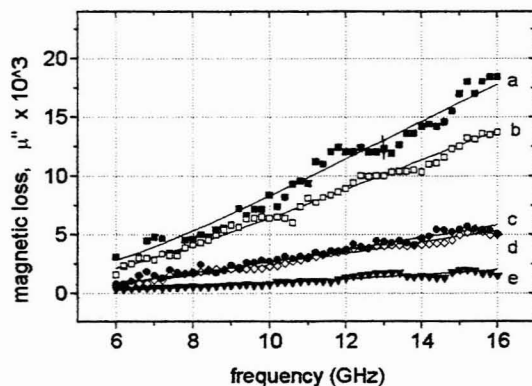


Figure 3b. Frequency dependence of magnetic loss  $\mu''$  for 5 selected snow samples

Model calculations for snow magnetic permeability have been done based on the concept of electrically conducting water rings around contact zones of ice grains. Due to surface tension

water may be arranged in pendular menisci as shown in Fig.4a; for simplicity of mathematical calculations, water menisci in the snow pendular regime have been replaced by toroidal shaped rings, Fig.4b.

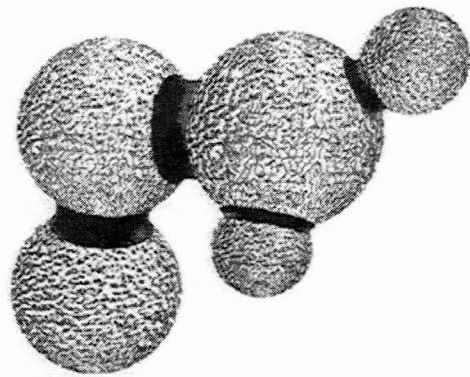


Figure 4a. Arrangement of water menisci in a cluster of ice grains

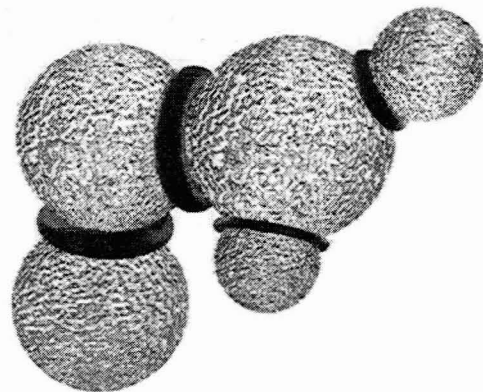


Figure 4b. Model of snow pendular regime: Water rings in a cluster of ice grains

The electric current  $I$  in the rings is driven by the induced electric field (according to Faraday's Law of induction), and depends on the actual conductivity and self-inductance of the current loop. For the present model calculations it is assumed, that conductivity  $\sigma$  is dominated by  $\epsilon''$ , the dielectric loss of water with a maximum in the X-band regime; the ionic contribution to the total conductivity, however, can be neglected:  $\sigma \approx \omega \cdot \epsilon_0 \cdot \epsilon''$ ,  $\omega$  the frequency in rad/s. The magnitude of the total 'induced' magnetic dipole density  $p$  is given by:  $p = \frac{1}{2} \cdot W_r \cdot I \cdot a / A$ ,  $W_r$  the fraction of total water volume collected in pendular rings,  $a$  the ring radius, and  $A$  the ring cross-section. Assuming an isotropic distribution of pendular water rings,

the 'induced' complex magnetic permeability can be calculated from  $p$  according to:

$$\mu = 3 / [3 - i.N / (1-i.M)] \quad (1)$$

with  $N = \frac{1}{4}.W_r. \epsilon'' . [a.\omega/c]^2$ , and  $M = 2.\pi.[f/c]^2.\epsilon'' . A.[\ln(8.a/b)-2]$ ,  $a$  and  $b$  the torus radii (Ahammer, 1996).

A calculation of the water volume  $V_r$  contained in menisci around contact zones of spherical ice grains of radius  $r$  has recently been given by Frankenfield (1996):

$V_r = (4/3).\pi.r^3.f(\varphi, \Theta)$ . The function  $f(\varphi, \Theta)$  depends on the ring size  $\varphi$ , and the angle of contact between ice and water,  $\Theta$ . Ring water content  $W_r$  can be calculated according to:

$W_r = (1 - \Phi). f(\varphi, \Theta)$ ,  $\Phi$ : snow porosity. A graphical representation of  $f(\varphi, \Theta)$ , the ratio of ring-water volume to the ice-grain volume is given in Fig.5 for 2 limiting values of contact angle  $\Theta$ ,  $\Theta = 0^\circ$  and  $\Theta = 10^\circ$  (Hobbs, 1974).

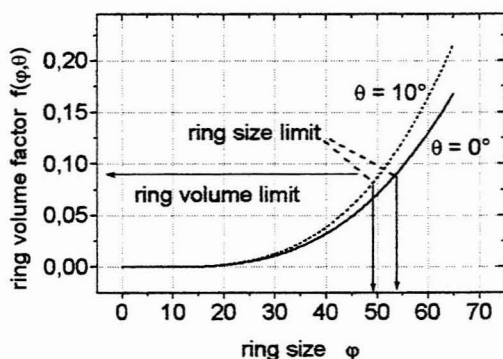


Figure 5. Ratio of ring-water volume to the ice-grain volume.

The ring volume limit (maximum ring size) is defined by zero capillary pressure difference across the wetting and non-wetting boundary, and this allows an estimation of the upper limit for the existence of pendular water rings:  $f(\varphi, \Theta) \leq 0.09$ ,  $W_r < 5\%$  for 50% porosity.

Consequently, it is expected that magnetic effects may only be observed with low to moderate wet and coarse grained snow.

#### 4. EXPERIMENTAL RESULTS

The magnetic permeability of a total of 31 snow samples has been measured in the frequency range of 12 up to 16 GHz, for selected samples the measurement range has

been extended from 8 up to 16 GHz or from 6 up to 16 GHz, respectively. Model calculations of permeability  $\mu$  have been done according to Equ.(1), whereby the fraction of total water which is arranged in pendular rings,  $W_r$ , has been used as a fitting parameter. Indications of drastic effects of small changes in snow water content on water geometry can be seen in Fig.6: magnetic loss for 2 selected snow samples, sample b and f, which differ only in water saturation, is shown in the 8 to 16 GHz range together with a model calculation (solid lines). The apparent significant difference in magnetic response may be explained by a difference in water geometric arrangement: sample b seems to be well within the pendular regime,  $W_r \approx W_{tot}$ , sample f, however, may be in a transition between the pendular and funicular zone,  $W_r \ll W_{tot}$ . In contrast, samples c and d (Fig. 3b) differ significantly in the total water content, the difference in the magnetic losses,  $\mu''$ , however, is very low: This may also be explained by a specific difference in water geometry and the difference in grain size. Characteristic data of these snow samples are given in Table 2.

sample	$W_{tot}$ [%]	$\Phi$ [%]	$r$ [mm]	$W_r$ [%]
b	4.7	52	1.3	4.1
f	5.5	45	1.2	1.0
c	5.1	46	1.5	1.3
d	2.2	47	1.1	2.2

Table 2. Characteristic data of selected snow samples, samples b, c, d and f.

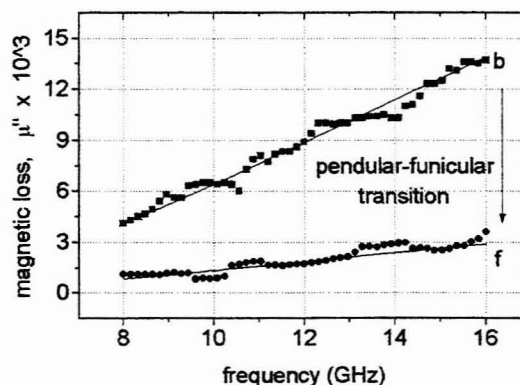


Figure 6. Magnetic losses at the pendular-funicular transition. Data points are shown together with model calculations (solid lines).



The dependence of magnetic loss on total water content is shown in Fig.7 for a selected frequency of 14 GHz. For comparison, measured magnetic data have been normalized to a standard mean grain-size of  $r = 1\text{mm}$ :  $M'' := \mu'' / r^2$ . The solid line represents a model calculation based on the assumption  $W_r = W_{\text{tot}}$ . For a total

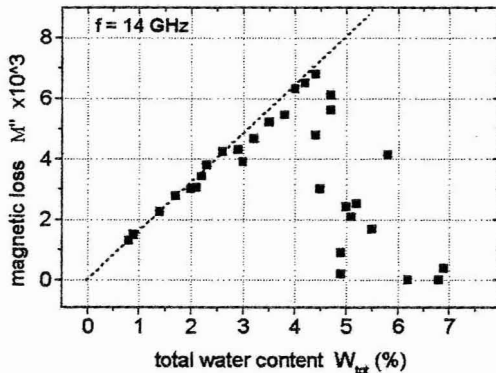


Figure 7. Dependence of normalized magnetic loss on total water content.

water content up to approximately  $W_{\text{tot}} \approx 4.5\%$ , more or less all the free water may be arranged in ring-like structures, although deviations can be observed for  $W_{\text{tot}} > 3\%$ . For water contents exceeding a critical value of  $\approx 4.5\%$ , magnetic losses decrease significantly and the material snow approaches its intrinsic very low natural diamagnetism. The decrease in magnetic response may be due to a merging of water rings forming closed spheroidal water bodies or forming a more or less continuous water phase. In Fig.8, the fraction of water which is arranged in ring-like structures,  $S_r$ , is shown against total water content,  $S_{\text{tot}}$ , whereby, for comparison, water content has been related to snow porosity:  $S_r = W_r / \Phi$ , and  $S_{\text{tot}} = W_{\text{tot}} / \Phi$ . The zone, where most of the water component may be arranged in ring-shaped configurations, the pendular zone, extends from zero saturation to approximately  $S_{\text{tot}} \approx 8\%$ , it is followed by a transitional zone in the range of  $8\% \leq S_{\text{tot}} \leq 13\%$  and by the funicular zone at higher saturations. This compares favorably with dielectric (Colbeck, 1982; Denoth, 1982a) and also hydraulic measurements (Denoth, 1980).

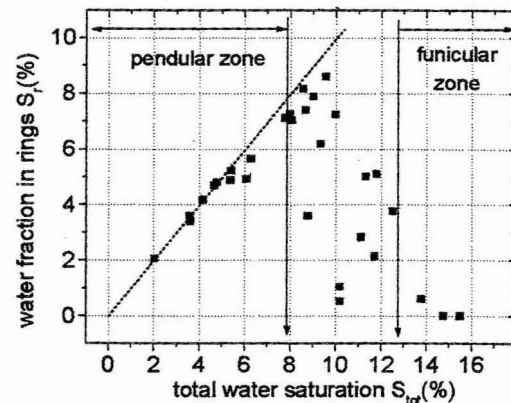


Figure 8. Dependence of water fraction in ring-like structures on total water saturation.

## 5. CONCLUSION

Measurements of the magnetic response of moderate wet coarse-grained Alpine snow samples confirm the existence of closed ring-shaped water bodies in the pendular regime. The pendular regime extends to a saturation of approximately 8% of the pore volume, and the transition to the funicular mode occurs in a relatively narrow transitional zone where the water bodies re-arrange. Compared to the dielectric response of wet snow, the magnetic response is relatively weak: it can only be observed at low wetness and with large ice grains. So, for practical applications, the consideration of magnetic effects in wet snow may be neglected.

## ACKNOWLEDGEMENTS

The 'Österreichische Forschungsgemeinschaft' is thanked for supporting in part presentation through grant no. 06/5255. My son Dietmar is thanked for drawing Figures 4a and 4b, an artist-like view of snow pendular regime.

## REFERENCES

- Achammer, T., 1996: Untersuchungen ueber das elektromagnetische Verhalten poroesser, koemiger Materialien im Mikrowellenbereich. Thesis, Univ. Innsbruck.

- Azzam, R.M.A, and N.M. Bashara, 1979: Ellipsometry and polarized light. North-Holland Publishing Comp.: Amsterdam, NewYork.
- Colbeck, S.C., 1982: The geometry and permittivity of snow at high frequencies. *J. Appl.Phys.* 53(6), 4495-4500
- Denoth, A., 1980: The pendular-funicular liquid transition in snow. *J.Glac.* 25, 91, 93-97
- Denoth, A., 1982a: The pendular-funicular liquid transition and snow metamorphism. *J.Glac.*, 28, 99, 357-364
- Denoth, A., 1982b: Effect of grain geometry on electrical properties of snow at frequencies up to 100 MHz. *J.Appl.Phys.*, 53, 11, 7496-7501
- Denoth, A., 1994a: An electronic device for long-term snow wetness recording. *Annals Glac.*, 19, 104-106
- Denoth, A., 1994b: Snow liquid water measurements: Methods, Instrumentation, Results Proc. Symp. on Snow and Related Manifestations. Manali, India, 150-153
- Frankenfield, J., 1996: Pore-space characterization of wet snow in the pendular regime. Proc. ISSW'96, Banff, Canada, 163-164
- Gunter, R., 1990: Modern Optics. J. Wiley & Sons, New York.
- Hallikainen, M., F.T. Ulaby, and M. Abdelrazik, 1984: The dielectric behaviour of snow in the 3 to 37 GHz range. IEEE Geosci. Remote Sensing Symp., Strasbourg, France, 169-176
- Hobbs, P.,V., 1974: Ice Physics. Clarendon Press, Oxford.
- Mätzler, C., 1988: Eddy currents in heterogeneous mixtures. *J. Electromagn. Waves and Applications*, 2, 5/6, 473-479
- Polder, D. and J.H. van Santen, 1946: The effective permeability of mixtures of solids. *Physica* 12, 5, 257-271
- Scheidegger, A. E., 1974: The physics of flow through porous media. Univ. of Toronto press.